

## Accepted Manuscript

Olive Secoiridoids and Semisynthetic Bioisostere Analogues for the Control of Metastatic Breast Cancer

Belnaser A. Busnena, Ahmed I. Foudah, Tina Melancon, Khalid A. El Sayed

PII: S0968-0896(13)00027-8  
DOI: <http://dx.doi.org/10.1016/j.bmc.2012.12.050>  
Reference: BMC 10518

To appear in: *Bioorganic & Medicinal Chemistry*

Received Date: 18 October 2012  
Revised Date: 19 December 2012  
Accepted Date: 28 December 2012

Please cite this article as: Busnena, B.A., Foudah, A.I., Melancon, T., El Sayed, K.A., Olive Secoiridoids and Semisynthetic Bioisostere Analogues for the Control of Metastatic Breast Cancer, *Bioorganic & Medicinal Chemistry* (2013), doi: <http://dx.doi.org/10.1016/j.bmc.2012.12.050>

This is a PDF file of an unedited manuscript that has been accepted for publication. As a service to our customers we are providing this early version of the manuscript. The manuscript will undergo copyediting, typesetting, and review of the resulting proof before it is published in its final form. Please note that during the production process errors may be discovered which could affect the content, and all legal disclaimers that apply to the journal pertain.



**Olive Secoiridoids and Semisynthetic Bioisostere Analogues for the Control of  
Metastatic Breast Cancer**

**Belnaser A. Busnena, Ahmed I. Foudah, Tina Melancon, and Khalid A. El Sayed\***

*Department of Basic Pharmaceutical Sciences, College of Pharmacy, University of Louisiana at  
Monroe, Monroe, LA 71201.*

\* To whom Correspondence should be addressed. Telephone 318-342-1725. Fax: 318-342-1737.  
E-mail: [elsayed@ulm.edu](mailto:elsayed@ulm.edu)

**ABSTRACT**

(-)-Oleocanthal (**1**) and ligstroside aglycone (**2**) are common bioactive olive oil secoiridoids. Secoiridoid **1** has been previously reported as a c-MET inhibitor. Chemically, (-)-oleocanthal is the elenolic acid ester of the common olive phenolic alcohol tyrosol. Therefore, several analogues (**4-13**) were synthesized by esterification and carbamoylation of tyrosol using diverse phenolic naturally occurring in olive and heterocyclic acids as elenolic acid bioisosteres to assess the effect of replacing the acid moiety of (-)-oleocanthal. Their c-MET inhibitory activity as well as their antiproliferative, antimigratory, and anti-invasive activities against the highly metastatic human breast cancer cell line MDA-MB231 has been assessed. Ligstroside aglycone (**2**) showed the best antimigratory activity. Generally, tyrosol esters showed better activities versus carbamate analogues. Tyrosol sinapate (**5**) showed the best c-MET phosphorylation inhibitory activity in Z'-LYTE™ Kinase Assay. Both **1** and **5** competitively inhibited the ATP binding into its pocket in the c-MET catalytic domain. **5** showed selective activities against tumor cells without toxicity to the non-tumorigenic human breast MCF10A epithelial cell line. Tyrosol esters with a phenolic acid containing hydrogen bond donor and/or acceptor groups at the *para*-position have better anticancer and c-MET inhibitory activities. Olive oil secoiridoids are excellent scaffolds for the design of novel c-MET inhibitors.

**Keywords** Antimigratory, Anti-invasive, Antiproliferative, Breast cancer, Carbamoylation, c-MET, Esterification, Olive secoiridoids, Tyrosol sinapate, Wound-healing.

## 1. Introduction

c-MET is a tyrosine kinase receptor which is normally activated by its natural ligand hepatocyte growth factor (HGF). c-MET/HGF pathway is critical for the normal cellular development and hemostasis. Aberrant activation of this pathway involved in many cancer types, which triggers diverse pathways inducing cell migration, motility, proliferation, cell differentiation, and angiogenesis.<sup>1,2</sup> Inhibiting c-MET kinase domain activation is among strategies to target c-MET/HGF axis.<sup>1,2</sup> The Mediterranean diet is associated with beneficial health properties, including lower incidences of cardiovascular disease, age related cognitive disease, and cancer.<sup>3</sup> The Mediterranean countries have lower cancer incidence compared to the rest of European countries and the United States. This includes reduced rates of the large bowel, breast, endometrial, and prostate malignancies, which is attributed to the dietary practices; apart from possible genetic factors.<sup>4</sup> Olive oil is a key ingredient of the Mediterranean diet. In addition to its unsaturated fatty acids, it is rich in other minor phenolics. These phenolics include simple phenols, phenolic acids, flavonoids, lignans, and secoiridoids. Tyrosol (**3**) is the major olive phenolic either as free phenolic alcohol or in combination as in secoiridoids including (-)-oleocanthal (**1**), oleuropein aglycone, and ligstroside aglycone (**2**). Secoiridoid **1** recently reported to inhibit the c-MET kinase phosphorylation with IC<sub>50</sub> value of 4.8 μM.<sup>5</sup> It also inhibited the proliferation, migration, and invasion of the human breast and prostate cancer cell lines MCF7, MDA-MB231, and PC-3, respectively. On the other hand, **2** induced potent tumoricidal effects by selectively triggering high levels of apoptotic cell death in HER2-overexpressing breast carcinoma and showed moderate cytotoxicity against a panel of 39-human cancer cell lines, in vitro.<sup>6,7</sup> The alcohol moiety of both secoiridoids **1** and **2** is **3**. Based on the activity of **1** as a c-MET inhibitor, this study reports the synthesis of eight new and two

known tyrosol ester and carbamate analogues (**4-13**). Design of these analogues was based on replacing the **1**'s elenolic acid moiety with different bioisosteres, including natural olive-derived phenolic acids, synthetic heteroaromatic, and diverse aromatic isocyanates. The c-MET phosphorylation inhibitory activity was evaluated using Z'-LYTE™ Kinase Assay-Tyr6 Peptide kit. Both **1** and **5** proved ATP-competitive c-MET phosphorylation inhibitors using the Omnia® Kinase assay. The binding mode of **5** at the ATP binding site of three different crystal structures of c-MET kinase domain (PDB code: 3I5N, 3CD8, 2WD1) was studied in-silico. The antimigratory, antiproliferative, and anti-invasive activities of all compounds were evaluated against the highly metastatic human mammary epithelial breast cancer cell line MDA-MB231. Toxicity of all analogues was also evaluated against the non-tumorigenic human breast epithelial cell line MCF10A to assess their selectivity.

## 2. Results and discussion

### 2.1 Chemistry

Five new (**4**, **6-8**, and **10**) and two known ester analogues (**5** and **9**) were semisynthesized via the highly chemoselective Mitsunobu esterification of **3** with different olive-derived phenolic acids and nalidixic acid to generate the corresponding esters in 60-80% yields (Scheme 1). Tyrosol sinapate (**5**) was synthesized in 2007 to assess its antimicrobial activity and ability to protect the cultured cells from H<sub>2</sub>O<sub>2</sub>-induced oxidative damage and consequent apoptosis.<sup>8</sup> Tyrosol caffeate (**9**) was synthesized in 2005 to evaluate its effect on stimulus-induced reactive oxygen species production in human neutrophils.<sup>9</sup> The activity of **5** and **9** on the c-MET and its related anticancer activities have never been reported. In addition, three new carbamate analogues **11-13** were synthesized via the reaction of **3** with benzyl and *p*-tosyl isocyanates to

generate their corresponding carbamates in 60-70% yields (Scheme 2). Their identity was confirmed by analyses of their  $^1\text{H}$  and  $^{13}\text{C}$  NMR (Tables 1-4) and HREIMS data.

The HREIMS of **4** showed an  $[\text{M}+\text{H}]^+$  peak at  $m/z$  318.1103, suggesting the molecular formula  $\text{C}_{17}\text{H}_{18}\text{O}_6$  and possible ester analogue of **3**. The  $^1\text{H}$  NMR data of **4** (Table 1) showed the downfield shifting of the methylene  $\text{H}_2\text{-1}'$  ( $\delta$  4.41,  $\Delta\delta+0.74$ ), compared to that of **3**, suggesting possible esterification of the primary alcohol C-1'. Esterification was further confirmed by  $^{13}\text{C}$  NMR analysis, showing the downfield ester carbonyl C-1 ( $\delta$  166.7, Table 2). NMR data of **4** also showed typical aromatic and methoxy signals for the syringic acid moiety. The methylene triplet  $\text{H}_2\text{-1}'$  showed a  $^3J\text{-HMBC}$  correlation with the ester carbonyl C-1, confirming the identity of **4** as tyrosol syringate. The structure identity of each of esters **5-10** was similarly confirmed via extensive analyses of their spectral data (Tables 1-4 and Supporting Information).

Reaction of **3** with benzyl isocyanate afforded **11** and **13**. The HREIMS of **11** suggested the molecular formula  $\text{C}_{16}\text{H}_{17}\text{NO}_3$  and possible monocarbamoyl analogue of **3**. The downfield shifting of the methylene  $\text{H}_2\text{-1}'$  ( $\delta_{\text{H}}$  3.81,  $\Delta\delta+0.14$ ), compared to that of **3**, suggested possible carbamoylation of the primary alcohol C-1'. Carbamoylation was further confirmed in  $^{13}\text{C}$ -PENDANT spectrum through the downfield carbamate carbonyl C-1 ( $\delta_{\text{C}}$  156.2, Table 4). The  $^1\text{H}$  and  $^{13}\text{C}$  NMR data of **11** (Tables 3 and 4) also showed typical monobenzyl carbamoyl signals. The methylene triplet  $\text{H}_2\text{-1}'$  and  $\text{H}_2\text{-2}$  ( $\delta_{\text{H}}$  4.23) showed  $^3J\text{-HMBC}$  correlation with the carbamate carbonyl C-1, confirming the identity of **11** as tyrosol monobenzyl carbamate.

The HREIMS of **13** suggested the molecular formula  $\text{C}_{24}\text{H}_{24}\text{N}_2\text{O}_4$  and possible dibenzyl carbamoyl analogue of tyrosol. The NMR data of **13** was similar to **11** with additional benzyl carbamoyl moiety. The downfield shift of the aromatic protons H-4'/H8' and H-5'/H-7', in

addition to the upfield shifting of C-6' ( $\delta_C$  149.6) suggested the location of the second benzyl carbamoyl moiety on C-6'. The benzylic methylene doublet ( $\delta_H$  4.34) showed a  $^3J$ -HMBC correlation with the carbamate carbonyl C-1" ( $\delta_C$  155.2), confirming the identity of **13** as tyrosol dibenzylcarbamate. Analysis of the HREIMS and NMR data of **12** (Tables 3 and 4) proved its identity as tyrosol *p*-tosyl carbamate (Supporting Information).

## 2.2. Biological Activity

The antimigratory, antiproliferative, cytotoxic, and anti-invasive activities of **2-13** were evaluated using wound-healing (WHA), MTT, and Cultrex BME assays, respectively, against the highly metastatic human breast cancer MDA-MB231 cell line. The MTT cytotoxicity assay was also evaluated using the non-tumorigenic human breast epithelial cell line MCF10A. The Z'-LYTE™ Kinase Assay kit was used to evaluate the inhibitory activity of **2-13** against c-MET phosphorylation and compare their activity versus **1**. The kinetics of the c-MET phosphorylation inhibition of **1** and the most active bioisosteric analogue **5** has been assessed by Omnia® kinase assay.

### 2.2.1. Wound healing assay (WHA)<sup>5</sup>

The wound-healing assay is a simple method for the in vitro study of the directional cell migration. Generally, all tyrosol analogues showed better antimigratory activities than their parent alcohol **3**, but less activity than the natural secoiridoids **1** and **2**. Figure 1 shows the effect of the natural secoiridoid **2** and the phenolic alcohol **3** on the cell migration across the wound inflicted in the MDA-MB231 cell monolayer compared to the vehicle control and a 10  $\mu$ M dose of **1** as a positive control.<sup>5</sup> Tyrosol (**3**) showed no activity even at 50  $\mu$ M dose unlike **2**, which showed about 60% inhibition of the cell migration at 25  $\mu$ M dose. The calculated IC<sub>50</sub> value of **2** was 13.8  $\mu$ M. This clearly highlights the importance of the acylating acid and ester

pharmacophore in olive-derived secoiridoids for the antimigratory activity. The concentration of **1-13** that results in 50% inhibition of the cell migration,  $IC_{50}$ , is reported in Table 6. The most active semisynthetic analogue, **4**, showed better activity at 25  $\mu\text{M}$  dose with 60% inhibition of the cell migration compared to the other analogues (Figure 2). Its  $IC_{50}$  value was found to be 19.4  $\mu\text{M}$ . Esters **5** and **6** were slightly more active than **7** at 25  $\mu\text{M}$  dose, suggesting the importance of the hydrogen bond donor binding role of the hydroxyl groups of the acylating acid's aromatic ring. The activity of **5** was comparable to its c-MET phosphorylation inhibitory activity. Meanwhile, although **2** and **4** were the most active in the wound-healing assay, they showed weak c-MET activities, suggesting different molecular target(s) for their antimigratory effect.

### 2.2.2. Invasion assay<sup>23</sup>

The anti-invasive activity of compounds **1-10**, **12**, and **13** were evaluated in the Cultrex<sup>®</sup> BME cell invasion assay against the highly metastatic MDA-MB231 human breast cancer cell line (Figure 3). The natural product **1** was used as a positive drug control.<sup>5</sup> In a preliminary screening at two different doses, 10 and 20  $\mu\text{M}$ , tyrosol nalidixate (**10**) have shown the most potent activity, allowing only 60 and 36 % invasion, respectively. In addition, **2**, **5**, and **9** have shown more than 50 % inhibition of invasion at 20  $\mu\text{M}$ . At this dose, analogues with carbonyl group directly attached to the heterocyclic ring as in **10** inhibited the cell invasion better than analogues with one carbon separating the carbonyl ester and the heterocyclic ring as in **2**. Removing or replacing the heterocyclic with aromatic ring decreased the activity as represented by **1**, **4-9**, and **12-13**. Additional carbons between the ester carbonyl and aromatic ring, in addition to a *para*-hydroxyl group substitution at the aromatic ring can be alternative structural feature to replace the heterocyclic ring and maintain the activity as represented by **5** and **9**. The

activity level of **5** was parallel to its c-MET activity. Meanwhile, although the natural product **2** and the semisynthetic esters **9** and **10** were the most active in invasion assay, their weak c-MET activity suggests molecular target(s) different from c-MET for their anti-invasive activity.

### 2.2.3. MTT assay<sup>10,11</sup>

The MTT assay allows the measurement of cell viability and proliferation of cell populations in a quantitative colorimetric fashion by utilizing cellular ability to reduce the MTT reagent to insoluble purple formazan dye. In this assay, each analogue was tested at four concentrations; 25, 50, 75, and 100  $\mu\text{M}$ . The concentration of each analogue that resulted in 50% cell growth inhibition ( $\text{IC}_{50}$ ) was measured (Table 6). The natural olive secoiridoid **2** and the c-MET inhibitor **5** were the most active antiproliferative analogues with  $\text{IC}_{50}$  values of 80.4 and 73.7  $\mu\text{M}$ , respectively (Figure 4). The cytotoxic effect of all compounds **2-13** was tested against the human mammary epithelial breast cancer cell line MDA-MB231. This experiment enabled the confirmation of the fact that the antimigratory activity was not due to the cytotoxic effects of tested compounds on MDA-MB231. All compounds were non-toxic at 50  $\mu\text{M}$  except **10**, which was cytotoxic at this concentration. In addition, the toxicity of the most active analogues in both WHA and MTT proliferation assays was assessed using MTT assay against the non-tumorigenic human breast cell line MCF10A (Figure 5). All active analogues were non-toxic at concentrations equal to their  $\text{IC}_{50}$  in both WHA and MTT proliferation assay, suggesting their good selectivity toward the malignant cells.

### 2.2.4. Z'-LYTE™ c-MET kinase assay<sup>12</sup>

The Z'-LYTE™ Kinase Assay-Tyr6 Peptide kit (Invitrogen) was used to assess the in vitro ability of **2**, **3**, and the semisynthetic analogues **4-13** to inhibit the c-MET phosphorylation. Meanwhile, **1** was used as a positive standard control for activity comparison.<sup>5</sup> Table 5 shows the

percentage of phosphorylation inhibition at a single 25  $\mu\text{M}$  dose concentration for **1-13** except **1**, which was used at a 10  $\mu\text{M}$  dose.<sup>5</sup> Ester **5** was the most potent c-MET phosphorylation inhibitor, with an  $\text{IC}_{50}$  value of 13.7  $\mu\text{M}$  (Figure 6). The remarkable activity difference between **3** and **5** in the c-MET inhibitory activity indicated the importance of the phenolic functionality in the acidic part for binding. The importance of C-7 free phenolic hydroxy group for the c-MET activity was highlighted by the complete activity loss of **7**, which is the C-7 methyl ether of **5**. This clearly indicated the HBD role for the c-MET activity of **5**. The reduced activity of carbamates suggests the preference of the ester pharmacophore for better c-MET activity. (-)-Oleocanthal (**1**) remained the most potent c-MET inhibitor, compared to **2** and tyrosol esters or carbamates, indicating the preference of elenolic acid over the rest of olive-derived phenolic acids. The calculated  $\text{IC}_{50}$  of **1** in this assay was 5.5  $\mu\text{M}$ , which was consistent with the reported value (4.8  $\mu\text{M}$ ),<sup>5</sup> validating this study's results.

### 2.2.5. Omnia<sup>®</sup> kinase assay<sup>13</sup>

Omnia<sup>®</sup> kinase Assay-Tyr12 peptide kit (Invitrogen) was used to assess the kinetic modality of analogue **5** as c-MET inhibitor. We studied the Michaelis-Menten parameters  $K_m$  and  $V_{\text{max}}$  of an enzymatic reaction in presence of **5** (20, 10, and 5  $\mu\text{M}$ ) to determine the mode of action of this c-MET inhibitor. The maximum observed velocity at enzyme saturating substrate concentration is designated as  $V_{\text{max}}$ . Michaelis-Menten constant,  $K_m$  is the substrate concentration that produces half-maximal velocity. Tyrosol sinapate (**5**) nearly did not affect the  $V_{\text{max}}$  at the end of experiment while the  $K_m$  was increased (Figure 7). This pattern is well known for the competitive inhibitors. To validate this assay, the known c-MET competitive inhibitor SU11274 has been used as a positive control at 100 and 25 nM concentrations and showed typical ATP competitive inhibitor pattern (Figure 7).<sup>14</sup> Similarly, (-)-oleocanthal (**1**) showed

ATP-competitive c-MET inhibitory pattern, validating the previously reported in-silico conclusion.<sup>5</sup>

### 3. Molecular docking study

About 20 c-MET crystal structures were published with and without ligands, revealing two distinct binding modes for ATP-competitive inhibitors. Type I ligands assume U-shape geometry through interactions with hinge region Met1160 and activation loop residue Tyr1230, unlike type II ligands, which adopt extended orientation.<sup>15-17</sup> c-MET ATP binding site includes: 1) Hinge region: Met1160 and Pro1158. Interaction at this site is highly characteristic for all compounds targeting the ATP binding site.<sup>5,15</sup> 2) Central hydrophobic region. 3) Two hydrophobic subpockets. 4) c-MET activation loop (Asp1222-Lys1245).<sup>15-17</sup>

(-)-Oleocanthal (**1**) was identified via a computer-assisted study as a c-MET activation inhibitor hit, targeting its ATP binding site, and stabilizing the kinase domain in its inactive conformation.<sup>5</sup> Docking of **1** into the ATP binding site of c-MET crystal structure PDB: 3I5N demonstrated the formation of a hydrogen bond (HB) between **1**'s phenolic hydroxyl group and both of Pro1158 and Met1160.<sup>5</sup> Two additional HBs observed between **1**'s C-1 aldehyde and Tyr1230 and Arg1086. **1** Filled the space between the hinge region and activation loop (Pro1158/Asn1167-Tyr1230).<sup>5</sup> The ester moiety was hypothesized not to contribute any binding role yet it provided the proper molecular size and confirmation for adequate binding. A slightly similar binding mode of **1** was noted with another c-MET crystal structure (PDB: 1R0P).<sup>5</sup> Both binding modes suggested that **1** can fully fit at the ATP binding site of the c-MET, which was experimentally proved in this study.

In this study, three highly resolved c-MET kinase domain crystal structures (PDB: 3I5N, 3CD8, 2WD1) with a resolution of 2Å were used to assess the binding mode of **5**, the most

active tyrosol analogue, at the c-MET's ATP binding pocket. Good binding affinity for any c-MET active hit is hypothesized to be through interactions with at least one of Asp1222, Phe1223, or Tyr1230 at the activation loop and either of Pro1158 or Met1160 at the hinge region.<sup>5,18</sup>

To validate the docking results, each of the c-MET's crystal structure 3I5N, 3CD8, and 2WD1 ligand (**14-16**, respectively) was docked into its ATP binding pocket by using the same parameters which have been used for docking analogue **5**. Each ligand was almost overlaid the original co-crystallized structure (Figure 8 and Supporting Information Figures 1.1 and 1.3).<sup>19-21</sup>

Tyrosol's C-6' phenolic hydroxyl of **5** exhibited two hydrogen bonding interactions (HB) with the hinge region's essential amino acids Met1160 and Pro1158 of the three c-MET crystal structures (Figure 8 and Supporting Information Figures 1.2 and 1.4). The MOLCAD visualization of the docked pose of **5** emphasized its complete fitting at the c-MET's ATP pocket.<sup>22</sup> Another HB interaction was observed between the aromatic C-7 phenolic hydroxyl group of sinapic acid with ASN1167 in both crystal structures 3I5N and 3CD8 (Figure 8A and Supporting Information Figure 1.2). Furthermore, a  $\pi$ - $\pi$  interaction has also been observed within 5 Å distance between the Tyr1230's aromatic ring at the activation loop and the sinapic acid's aromatic ring in crystal structure 2WD1 (Figure 8 and Supporting Information Figure 4).

#### 4. Conclusion

The natural secoiridoid **2** and the semisynthetic ester **4** were the most active in the wound-healing migration assay without any cytotoxicity to normal cells. They showed minimal c-MET inhibitory activity, which may indicate that their antimigratory activity could be via molecular target(s) other than the c-MET. Tyrosol sinapate (**5**) is a new ATP-competitive c-MET kinase phosphorylation inhibitory scaffold with antimigratory, antiproliferative, and anti-invasive

activities. It lacks cytotoxicity to the normal epithelial breast cells. Olive secoiridoids can be good scaffolds for the control of metastatic breast cancer and design of novel c-MET inhibitors.

## 5. Material and methods

### 5.1. General experimental procedures

The  $^1\text{H}$  and  $^{13}\text{C}$  NMR spectra were recorded in  $\text{CDCl}_3$  and using TMS as an internal standard on a JEOL Eclipse-400 NMR spectrometer, operating at 400 MHz for  $^1\text{H}$  and 100 MHz for  $^{13}\text{C}$  NMR. The HREIMS experiments were conducted at Louisiana State University on a 6200-TOF LC-MS (Agilent), equipped with a multimode source (mixed source that can ionize the compounds alternatively by ESI and APCI). Thin layer chromatography (TLC) analysis was carried on precoated Si gel 60 F<sub>254</sub> 500  $\mu\text{m}$  TLC plates (EMD Chemicals), using *n*-hexane-ethyl acetate (5:5) as a mobile phase. 1% Vanillin in concentrated  $\text{H}_2\text{SO}_4$  was used as a visualizing reagent. For column chromatography, Si gel 60 (Natland, 63–200  $\mu\text{m}$ ) and Sephadex LH-20 were used. A Dionex Summit III high performance liquid chromatography (HPLC) system with a variable wave length UV detector set to 230 nm was used. Separation was performed on a Phenomenex Cosmosil 5C<sub>18</sub>-AR-II column (250 mm x 4.6 mm, 5  $\mu\text{m}$ ; Phenomenex Inc., Torrance, CA) at 25 °C. Isocratic elution was performed using  $\text{H}_2\text{O}$ - $\text{CH}_3\text{CN}$  (6:4) as a mobile phase. A flow rate of 1mL/min, 25  $\mu\text{L}$  injection volume and 1 mg/mL sample concentration were used. Generally, 1:100 ratios of mixtures to be chromatographed versus used stationary phase were used in all liquid chromatographic purifications.

### 5.2. Compounds

(-)-Oleocanthal, tyrosol, and ligstroside aglycone were isolated from extra-virgin olive oil as described below. HPLC, was prepared and used as previously described.<sup>23,24</sup> SU11274 was

purchased from Sigma-Aldrich. Sinapic, syringic, caffeic, homovanillic, 3,4,5-trimethoxycinnamic, nalidixic, and 2,3-dihydroxyphenylacetic acids as well as *p*-toluenesulfonyl and benzyl isocyanates were purchased from VWR (Suwanee, GA).

### 5.3. Extraction and isolation of olive phenolics<sup>23,24</sup>

About 2L methanol and 3L extra-virgin olive oil (Member's Mark, Batch No. VF2 US011410, Italy) were mixed, and then *n*-hexane (2L) was added to the methanolic fraction and shaken twice in separating funnels. Dried methanolic layer was subjected to repeated medium pressure liquid chromatography (MPLC) in a 50 × 3 cm column on lipophilic Sephadex LH20 (Sigma Aldrich, bead size 25–100 μ) using CH<sub>2</sub>Cl<sub>2</sub>, then CH<sub>2</sub>Cl<sub>2</sub>-MeOH, gradient elution, followed by HPLC analysis to separate **1-3** (Supporting Information Figure 2). Identification and purity of these compounds were based on HPLC analysis on a preparative Cosmosil AR-II column (Waters, Milford MA, 250 mm x 20 mm) and comparison of their <sup>1</sup>H and <sup>13</sup>C NMR data with the literature.<sup>23,24</sup>

### 5.4. Chemical reactions

#### 5.4.1. Chemoselective esterification of tyrosol using Mitsunobu reaction<sup>25</sup>

To a cooled (0 °C) solution of freshly prepared tyrosol (138 mg, 1 mM) and phenolic acids (1 mM equivalent) in dry THF (3.5 mL) were added triphenylphosphine (280 mg, 1 mM) and diisopropylazodicarboxylate (208 μL, 1 mM). After stirring for 48 h at rt, the reaction was worked up by removal of the solvent, and the residue was partitioned between ethyl acetate and saturated NaHCO<sub>3</sub>. The organic phase was washed with brine, dried over anhydrous Na<sub>2</sub>SO<sub>4</sub>, and evaporated. The residue was purified on Sephadex LH-20 (35 mL after CH<sub>2</sub>Cl<sub>2</sub> swelling) using CH<sub>2</sub>Cl<sub>2</sub> to remove the Mitsunobu byproducts, followed by normal phase chromatography to isolate the esters **4-10**.

**5.4.2. 6'-Hydroxyphenethyl-5-hydroxy-4,6-dimethoxybenzoate (Tyrosol syringate, 4)**

Compound **4** was prepared in 60% yield by reaction of 138 mg of **3** with 198 mg of syringic acid. Colorless oil; IR  $\nu_{\max}$ (CDCl<sub>3</sub>) 3940, 3053, 1707, 1264, 898 cm<sup>-1</sup>; <sup>1</sup>H and <sup>13</sup>C NMR, see Tables 1 and 2; HREIMS  $m/z$  319.1173 [M+H]<sup>+</sup> (calcd for C<sub>17</sub>H<sub>19</sub>O<sub>6</sub>, 319.1181).

**5.4.3. (E)-6'-Hydroxyphenethyl-3-(7-hydroxyl-6,8-dimethoxyphenyl)acrylate (Tyrosol sinapate, 5)<sup>8</sup>**

Compound **5** was prepared in 85% yield by reaction of 138 mg of **3** with 224 mg of sinapic acid. Colorless amorphous powder; IR  $\nu_{\max}$ (CDCl<sub>3</sub>) 3747, 1702, 1514, 1263, 898 cm<sup>-1</sup>; <sup>1</sup>H and <sup>13</sup>C NMR, see Tables 1 and 2; HREIMS  $m/z$  345.1336 [M<sup>+</sup>H]<sup>+</sup> (calcd for C<sub>19</sub>H<sub>21</sub>O<sub>6</sub>, 345.1338).

**5.4.4. 6'-Hydroxyphenethyl-1'-(3,4-dihydroxyphenyl)acetate (6)**

Compound **6** was prepared in 50% yield by the reaction of 138 mg of **3** with 168 mg of 3,4-dihydroxyphenylacetic acid. Colorless oil; IR  $\nu_{\max}$ (CDCl<sub>3</sub>) 3882, 1725, 1517, 1257, 890 cm<sup>-1</sup>; <sup>1</sup>H and <sup>13</sup>C NMR, see Tables 1 and 2; HREIMS  $m/z$  311.0885 [M+Na]<sup>+</sup> (calcd for C<sub>16</sub>H<sub>16</sub>O<sub>5</sub>Na, 311.0895).

**5.4.5. (E)-6'-Hydroxyphenethyl-3-(6,7,8-trimethoxyphenyl)acrylate (7)**

Compound **7** was prepared in 60% yield by reaction of 138 mg of **3** with 238 mg of 3,4,5-trimethoxycinnamic acid. Yellowish white amorphous powder; IR  $\nu_{\max}$ (CDCl<sub>3</sub>) 3941, 3054, 1705, 1268, 903 cm<sup>-1</sup>; <sup>1</sup>H and <sup>13</sup>C NMR, see Tables 1 and 2; HREIMS  $m/z$  381.1347 [M+Na]<sup>+</sup> (calcd for C<sub>20</sub>H<sub>22</sub>O<sub>6</sub>Na, 381.1314).

#### 5.4.6. 6'-Hydroxyphenethyl-2-(6-hydroxyl-5-methoxyphenyl)acetate (Tyrosol homovanillate, **8**)

Compound **8** was prepared in 60% yield by reaction of 138 mg of **3** with 182 mg of homovanillic acid. Colorless oil; IR  $\nu_{\max}$  (CDCl<sub>3</sub>) 3748, 1728, 1264, 898, cm<sup>-1</sup>; <sup>1</sup>H and <sup>13</sup>C NMR, see Tables 1 and 2; HREIMS  $m/z$  325.1043 [M<sup>+</sup>Na]<sup>+</sup> (calcd for C<sub>17</sub>H<sub>18</sub>O<sub>5</sub>Na, 325.1052).

#### 5.4.7. (E)-6'-Hydroxyphenethyl-3-(7,8-dihydroxyphenyl)acrylate (Tyrosol caffeate, **9**)<sup>9</sup>

Compound **9** was prepared in 60% yield by reaction of 138 mg of **3** with 180 mg of caffeic acid. Colorless oil; IR  $\nu_{\max}$  (CDCl<sub>3</sub>) 3940, 1703, 1264, 898 cm<sup>-1</sup>; <sup>1</sup>H and <sup>13</sup>C NMR, see Tables 3 and 4.

#### 5.4.8. 6'-Hydroxyphenethyl-1-ethyl-7-methyl-1,4-dihydro-1,8-naphthyridine-3-carboxylate (Tyrosol nalidixate, **10**)

Compound **10** was prepared in 70% yield by reaction of 138 mg of **3** with 232 mg of nalidixic acid. Colorless amorphous powder; IR  $\nu_{\max}$  (CDCl<sub>3</sub>) 3747, 1722, 1264, 914 cm<sup>-1</sup>; <sup>1</sup>H and <sup>13</sup>C NMR, see Tables 3 and 4; HREIMS  $m/z$  353.1303 [M+Na]<sup>+</sup> (calcd for C<sub>20</sub>H<sub>20</sub>N<sub>2</sub>O<sub>4</sub>Na, 375.1321).

#### 5.4.9. Carbamoylation of tyrosol<sup>26</sup>

To solutions of tyrosol in toluene (2 mL), benzyl or *p*-tosyl (toluenesulfonyl) isocyanates 10  $\mu$ L of triethylamine (Et<sub>3</sub>N) were added. Each solution was separately stirred and refluxed for 3 h. Water (10 mL) was added and each reaction mixture was extracted with ethyl acetate (3x10 mL). Each ethyl acetate extract was dried over anhydrous Na<sub>2</sub>SO<sub>4</sub>, concentrated under vacuum, and subjected to Sephadex LH20 and Si gel 60 normal phase column chromatography. Reaction

of **3** with benzyl isocyanate afforded compounds **11** and **13** while the same reaction with *p*-tosyl isocyanate afforded **12**.

#### 5.4.10. 6'-Hydroxyphenethylbenzyl carbamate (**11**)

Compound **11** was prepared in 60% yield by reaction of 138 mg of **3** with 133 mg of benzyl isocyanate. Colorless powder; IR  $\nu_{\max}$  (CDCl<sub>3</sub>) 3940, 1727, 1264, 898 cm<sup>-1</sup>; <sup>1</sup>H and <sup>13</sup>C, see Tables 3 and 4; HREIMS  $m/z$  272.1296 [M+H]<sup>+</sup> (calcd for C<sub>16</sub>H<sub>18</sub>NO<sub>3</sub>, 272.1287).

#### 5.4.11. 6'-Hydroxyphenethyltosyl carbamate (**12**)

Compound **12** was prepared in 70% yield by reaction of 138 mg of **3** with 197 mg of *p*-toluenesulfonyl isocyanate. Colorless amorphous powder; IR  $\nu_{\max}$  (CDCl<sub>3</sub>) 3826, 1747, 1160, 817 cm<sup>-1</sup>; <sup>1</sup>H and <sup>13</sup>C NMR, see Tables 3 and 4; HREIMS  $m/z$  358.0737 [M+H]<sup>+</sup> (calcd for C<sub>16</sub>H<sub>17</sub>NO<sub>5</sub>SNa, 358.0725).

#### 5.4.12. 1',6'-Phenethyldibenzyl carbamate (**13**)

Compound **13** was prepared in 65% yield by reaction of 138 mg of **3** with 133 mg of benzyl isocyanate. Colorless amorphous powder; IR  $\nu_{\max}$  (CDCl<sub>3</sub>) 3940, 1727, 1264, 898 cm<sup>-1</sup>; <sup>1</sup>H and <sup>13</sup>C NMR, see Tables 3 and 4; HREIMS  $m/z$  406.1886 [M+2H]<sup>+</sup> (calcd for C<sub>24</sub>H<sub>26</sub>N<sub>2</sub>O<sub>4</sub>, 406.1893).

### 5.5. Molecular modeling and docking

Three-dimensional structure modeling was performed using the SYBYL-X Program Package,<sup>27</sup> installed on DELL desktop workstations equipped with a dual 2.0 GHz Intel® Xeon® processor running the Red Hat Enterprise Linux (version 5) operating system. Conformations of all compounds were generated using Confort™ conformational analysis. Energy minimizations

were performed using the Tripos force field with a distance-dependent dielectric and the Powell conjugate gradient algorithm with a convergence criterion of 0.01 kcal/ (mol Å). Partial atomic charges were calculated using the semiempirical program MOPAC 6.0 and applying the AM1. Surflex-Dock Program version 2.0 interfaced with SYBYL-X was used to dock all compounds at the ATP binding site of c-MET. Surflex-Dock employs an idealized active site ligand (protomol) as a target to generate putative poses of molecules or molecular fragments.<sup>28</sup> These putative poses were scored using the Hammerhead scoring function.<sup>29</sup> The 3D structures (PDB: 3I5N, 3CD8, 2WD1) were taken from the Research Collaboratory for Structural Bioinformatics Protein Data Bank (<http://www.rcsb.org/pdb>).

## 5.6. Cell culture

Breast cancer and non-tumorigenic cell lines, MDA-MB231 and MCF10A, respectively, were purchased from ATCC (Manassas, VA). The cell lines were grown in RPMI 1640 medium (GIBCO-Invitrogen, NY) with 10% fetal bovine serum (FBS) and supplemented with glutamine (2 mmol/L), penicillin G (100 µg/mL), and streptomycin (100 µg/mL) at 37 °C under 5% CO<sub>2</sub>.

### 5.6.1. Preparation of various dilutions of tested analogues for cell culture assays

A stock solution was prepared by dissolving each tested analogue in DMSO at a concentration of 50 mM for all assays. About 2 µL of each stock solution was transferred to 998 µL of serum-free medium to obtain 100 µM concentrations (0.2% DMSO). Serial dilutions were then conducted to obtain the desired concentrations for each assay. The negative control was prepared as follows: adding 2 µL DMSO to 998 µL serum-free media (MTT assay); adding 3 µL DMSO to 1497 µL serum-free media (WHA).

## 5.7. MTT proliferation assay

The antiproliferative activity of tyrosol and its analogues was tested in culture on the human mammary epithelial breast cancer cell line, MDA-MB231. Cell growth was measured using MTT kit (TACS™, Trevigen® Inc.). Cells in exponential growth were plated in a 96-well plate at a density of  $8 \times 10^3$  cells per well, and allowed to attach over-night at 37 °C under 5% CO<sub>2</sub>. Complete growth medium was then replaced with 100 µL of 5% RPMI fresh serum media (GIBCO-Invitrogen, NY) containing various doses (25, 50, 75, and 100 µM) of the specific test compound and incubation resumed at 37 °C under 5% CO<sub>2</sub>. After 48 h, the media was replaced and the cells retreated with compounds using 5% RPMI fresh serum media for another 24 h. The cells were refreshed with 100 µL RPMI fresh serum free media before adding MTT solution (50 µL/well) and re-incubated for 4 h. The color reaction was stopped by the addition of solubilization/stop solution (DMSO, 100 µL/well), and incubation at 37 °C was continued to ensure complete dissolution of the formazan product. Absorbance of the samples was determined at  $\lambda 570$  nm with an ELISA plate reader (BioTek, VT, USA).

#### **5.8. Cultrex® BME cell invasion assay**

Anti-invasive activities were measured using Cultrex® BME cell invasion assay.<sup>30</sup> About 50 µL of basement membrane extract (BME) coat was added per well of the top chamber. After an over-night incubation at 37 °C in a 5% CO<sub>2</sub> atmosphere, 50,000/50 µL of MDA-MB231 cells in 0.5% FBS RPMI medium were added per well of the top chamber. 150 µL of RPMI medium was then added to the lower chamber. Media contained 10% FBS and penicillin/streptomycin as well as fibronectin (1 µL/mL) and *N*-formyl-Met-Leu-Phe (10 nM) as chemoattractants. Tested compounds were prepared at 6X the desired concentration and 10 µL of each of the compounds was added per well of the top chamber. Cells were incubated at 37 °C under 5% CO<sub>2</sub>, which allowed for cell invasion from the top to the lower chamber. After 24 h, the top and bottom

chambers were aspirated and washed with washing buffer supplied within the kit. About 100  $\mu\text{L}$  of cell dissociation solution/calcein-AM solution was added to the bottom chamber and incubated at 37  $^{\circ}\text{C}$  under 5%  $\text{CO}_2$  for 1h. The cells internalize calcein-AM, and the intracellular esterases cleave the acetomethyl ester (AM) moiety to generate free calcein. Fluorescence of the samples was determined at  $\lambda_{\text{excitation}}$  485 nm and  $\lambda_{\text{emission}}$  528 nm using an ELISA plate reader (BioTek, VT, USA). The number of cells that invaded through the BME coat was calculated using a standard curve.

### 5.9. MTT cytotoxicity assay

The cytotoxic effects of the tyrosol analogues were tested in culture of the human mammary epithelial breast cancer cell line MDA-MB231 and the non-tumorigenic human breast MCF10A cell line. Cell growth was measured using MTT kit (TACS<sup>TM</sup>, Trevigen<sup>®</sup> Inc.). Cells in exponential growth were plated in a 96-well plate at a density of  $20 \times 10^3$  cells per well, and allowed to attach over-night at 37  $^{\circ}\text{C}$  under 5%  $\text{CO}_2$ . Complete growth medium was then replaced with 100  $\mu\text{L}$  of RPMI serum free medium and 0.5% RPMI serum medium (GIBCO-Invitrogen, NY) containing various doses (25, 50, 75, and 100  $\mu\text{M}$ ) of the tested compounds in case of MCF10A and MDA-MB231, respectively. After that, the incubation resumed at 37  $^{\circ}\text{C}$  under 5%  $\text{CO}_2$  for 24 h. The cells were then refreshed with 100  $\mu\text{L}$  RPMI fresh serum free media before adding the MTT solution (50  $\mu\text{L}$ /well) and re-incubated for 4 h. The color reaction was stopped by the addition of solubilization/stop solution (DMSO) (100  $\mu\text{L}$ /well), and incubation at 37  $^{\circ}\text{C}$  was continued to ensure complete dissolution of the formazan product. Absorbance of the samples was determined at  $\lambda$  570 nm with an ELISA plate reader (BioTek, VT, USA). The cytotoxicity  $\text{IC}_{50}$  of **2** against MDA-MB231 has been reported to be 67  $\mu\text{M}$ .<sup>7</sup>

### 5.10. Wound healing assay

MDA-MB231 cells were plated onto sterile 24-well plates and allowed to form a confluent cell monolayer per well (>95% confluence) over-night. Wounds were then inflicted in each cell monolayer using a sterile 200  $\mu$ L pipette tip. Media was removed and cells were washed twice with PBS and once with fresh serum free media. Test compounds at the desired concentrations in 0.5% fresh serum media were added to each well. The incubation was carried out for 24 h, after which media was removed and cells were washed, fixed and stained using Diff-Quick™ staining (Dade Behring Diagnostics, Aguada, Puerto Rico). Cells which migrated across the inflicted wound were counted under the microscope in three or more randomly selected fields (400X).<sup>31,32</sup>

#### 5.11. Z'-LYTE™ kinase assay

Z'-LYTE™ Kinase Assay-Tyr 6 Peptide kit (Invitrogen) was used to assess the ability of tyrosol analogues to inhibit c-MET phosphorylation. Briefly, 20  $\mu$ L/well reactions were set up in 96-well plates containing kinase buffer, 200  $\mu$ M ATP, 4  $\mu$ M Z'-LYTE™ Tyr6 Peptide substrate, 2500 ng/mL c-MET kinase and compound of interest as an inhibitor. After 1 h of incubation at rt, 10  $\mu$ L development solution containing site-specific protease was added to each well. Incubation was continued for 1 h. The reaction was then stopped, and the fluorescent signal ratio of 445 nm (coumarin)/520 nm (fluorescein) was determined on a plate reader (BioTek-FLx800™), which reflects the peptide substrate cleavage status and/or the kinase inhibitory activity in the reaction.

#### 5.12. Omnia® kinase assay

Omnia® kinase Assay-Tyr12 peptide kit (Invitrogen) was used to assess the kinetics of c-MET inhibitors. Assay reagents prepared as outlined by the manufacturer's manual.<sup>33</sup> The assay was performed in half-area 96-well plate (Perkin Elmer, Waltham, MA). The volume of reaction in each well was 40  $\mu$ L. For kinetics study, kinase (100 ng/well), SU11274 dilutions (100 and 25

nM), analogue **1** and **5** dilutions (20, 10, 5  $\mu$ M) were used. ATP concentrations used were: 1000, 800, 500, 333, 250, 200, 125, 100, 50 and 20  $\mu$ M. The peptide control Master Mix, phosphopeptide generation Master Mix, and kinetic reaction Master Mix as well as the assay steps were adopted according to the manufacturer's manual.<sup>30</sup> Reaction mixtures were then incubated for 60 min at 30 °C. The relative fluorescence units (RFU) data was collected every 70 seconds by fluorescence microplate reader (FLx800, Biotek Instruments, Inc.). The  $\Delta$ RFU was then calculated by subtracting the RFU value of peptide control wells (containing no kinase) from the RFU value of kinase reaction for each time point. The background was subtracted and  $\Delta$ RFU is plotted against time and log MET concentration. Curve-fitting to Michaelis-Menten equation was conducted using Prism 5.0 software from GraphPad Prism Software, Inc.

### Acknowledgment

The Libyan Government is greatly acknowledged for the fellowship support of B.B.

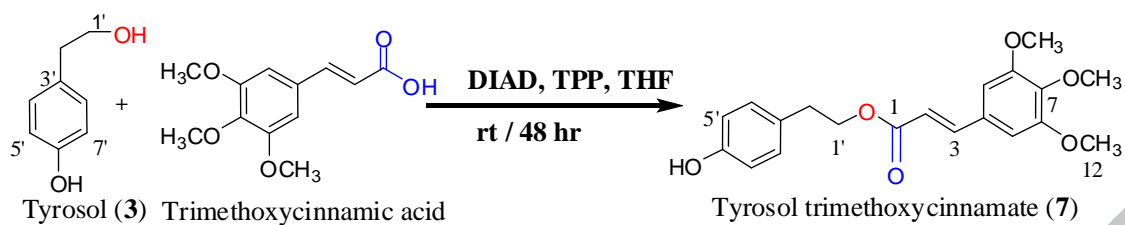
### References and notes

1. Satter, M.; Salgia, R. *Curr. Oncol. Rep.* **2007**, *9*, 102.
2. Liu, X.; Newton, C. R.; Scherle, A. P. *Expert Opin. Invest. Drugs.* **2011**, *20*, 1225.
3. Colomer, R.; Menendez, J. A. *Clin. Transl. Oncol.* **2006**, *8*, 15.
4. Lastra, C.; Barranco, M. D.; Motilva, V.; Herrerias, J. M. *Curr. Pharm. Des.* **2001**, *7*, 933.
5. Elnagar, A. Y.; Sylvester, P. W.; El Sayed, K. A. *Planta Medica.* **2011**, *77*, 1013.
6. Menendez, J. A.; Vazquez, A.; Garcia, R.; Carrasco, A.; Oliveras, C.; Fernandez, A.; Segura, A. *BMC Cancer.* **2008**, *8*, 377.
7. Kikuchi, M.; Uehara, Y.; Kikuchi, M.; Mano, N.; Machida, K. *J. Nat. Med.* **2011**, *65*, 237.

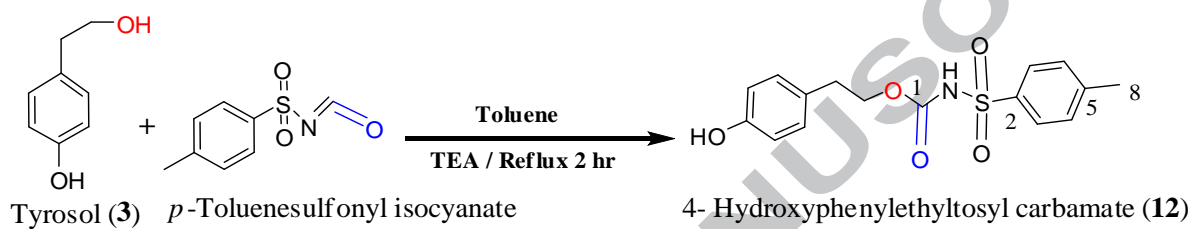
8. Stevenson, E. D.; Parkar, G. S.; Zhang, J.; Stanley, A. R.; Jensen, J. D.; Cooney, M. J. *J. Enzyme Microb. Technol.* **2007**, *40*, 1078.
9. Lee, Y. T.; Don, M. J.; Liao, C. H.; Chiou, H. W.; Chen, C. F.; Ho, L. K. *Clin. Chem. Acta.* **2005**, *352*, 135.
10. TACS™ MTT Cell Proliferation Assays Protocol; [www.trevigen.com](http://www.trevigen.com), accessed on 22/05/2011.
11. Mosmann, T. *J. Immunol. Methods.* **1983**, *65*, 55.
12. Rodems, S. M.; Hamman, B. D.; Lin, C.; Zhao, J.; Shah, S.; Heidary, D.; Makings, L.; Stack, J. H.; Pollok, B. A. *Assay Drug Dev. Technol.* **2002**, *1*, 9.
13. Shults, M. D.; Imperiali, B. *J. Am. Chem. Soc.* **2003**, *125*, 14248.
14. Berthou, S.; Aebersold, D. M.; Schmidt, L. S.; Stroka, D.; Heigl, C.; Streit, B.; Stalder, D.; Gruber, G.; Liang, C.; Howlett, A. R.; Candinas, D.; Greiner, R. H.; Lipson, K. E.; Zimmer, Y. *Oncogene* **2004**, *23*, 5387.
15. Schiering, N.; Knapp, S.; Marconi, M.; Flocco, M. M.; Cui, J.; Perego, R.; Rusconi, L.; Cristiani, C. *PNAS.* **2003**, *100*, 12654.
16. Wang, W.; Marimuthu, A.; Tsai, J.; Kumar, A.; Krupka, H. I.; Zhang, C.; Powell, B.; Suzuki, Y.; Nguyen, H.; Tabrizizad, M.; Luu, C.; West, B. L. *PNAS* **2006**, *103*, 3563.
17. Christensen, J.; Burrows, J.; Salgia, R. *Cancer Lett.* **2005**, *225*, 1.
18. Peach, L. M.; Tan, N.; Choyke, J. S.; Giubellino, A.; Athauda, G.; Burke, R. T., Jr.; Nicklaus, C. M.; Bottaro, P. D. *J. Med. Chem.* **2009**, *52*, 943.
19. Boezio, A. A.; Berry, L.; Albrecht, K. B.; Bauer, D.; Bellon, F. S.; Bode, C.; Chen, A.; Choquette, D.; Dussault, I.; Fang, M.; Hirai, S.; Kaplan, P.; Larrow, J. F.; Lin, J. M.; Lohman, J.;

- Potashman, H. M.; Rex, K.; Santostefano, M.; Shah, K.; Shimanovich, R.; Springer, K. S.; Teffera, Y.; Yang, Y.; Zhang, Y.; Harmange, J. *J. Bioorg. Med. Chem. Lett.* **2009**, *19*, 6307.
20. Albrecht, K. B.; Harmange, J.; Bauer, D.; Berry, L.; Bode, C.; Boezio, A. A.; Chen, A.; Choquette, D.; Dussault, I.; Fridrich, C.; Hirai, S.; Hoffman, D.; Larrow, J. F.; Kaplan, P.; Lin, J.; Lohman, J.; Long, M. A.; Moriguchi, J.; O'Connor, A.; Potashman, H. M.; Reese, M.; Rex, K.; Siegmund, A.; Shah, K.; Shimanovich, R.; Springer, K. S.; Teffera, Y.; Yang, Y.; Zhang, Y.; Bellon, F. S. *J. Med. Chem.* **2008**, *51*, 2879.
21. Porter, J.; Lumb, S.; Franklin, J. R.; Gascon, M. G.; Calmiano, M.; Le Riche, K.; Lallemand, B.; Keyaerts, J.; Edwards, H.; Maloney, A.; Delgado, J.; King, L.; Foley, A.; Lecomte, F.; Reuberson, J.; Meier, C.; Batchelor, M. *Bioorg. Med. Chem. Lett.* **2009**, *19*, 2780.
22. Heiden, W.; Goetze, T.; Brickmann, J. *J. Comp. Chem.* **1993**, *14*, 246.
23. Christophoridou, S.; Dais, P.; Tseng, L. H.; Spraul, M. *J. Agric. Food Chem.* **2005**, *53*, 4667.
24. Montedoro, G.; Servili, M.; Baldioli, M.; Selvaggini, R.; Miniati, E.; Macchioni, A. *J. Agric. Food Chem.* **1993**, *41*, 2228.
25. Appendino, G.; Minassi, A.; Daddario, N.; Bianchi, F.; Tron, G. *Org. Lett.* **2002**, *4*, 3839.
26. Hassan, M. H.; Elnagar, Y. A.; Khanfar, A. M.; Sallam, A. A.; Rabab, M.; Shaala, A. L.; Youssef, T. D.; Hifnawy, S. M.; El Sayed, A. K. *Eur. J. Med. Chem.* **2011**, *46*, 1122.
27. Tripos Associates. SYBYL Molecular Modeling Software, version 8.0; Tripos Associates: St. Louis, MO, **2007**; <http://www.tripos.com>, accessed on 08/18/2012.
28. Welch, W.; Ruppert, J.; Jain, A. *Chem. Biol.* **1996**, *3*, 449.
29. Jain, AN. *J. Med. Chem.* **2003**, *46*, 499.
30. Cultrex<sup>®</sup> BME Cell Invasion Assay Protocol; [www.trevigen.com](http://www.trevigen.com), accessed on 09/15/2012.

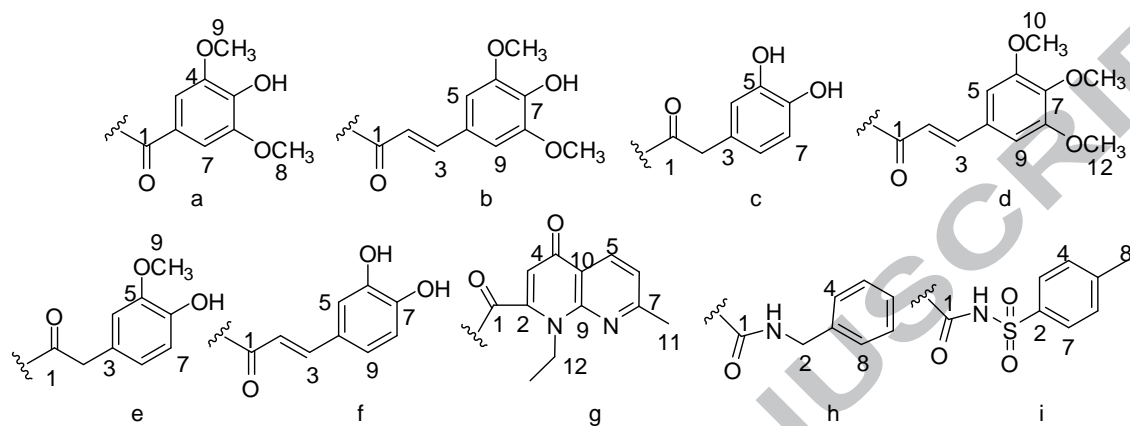
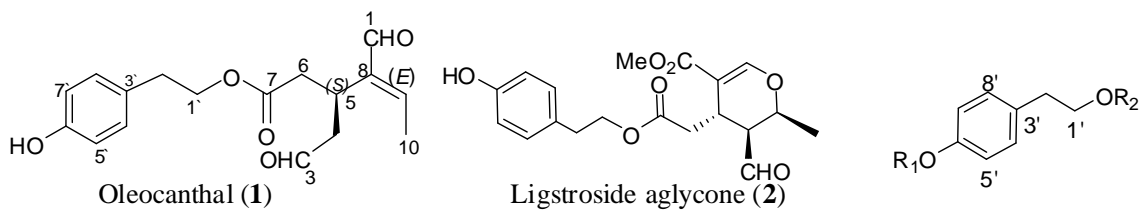
31. Mudit, M.; Khanfar, M.; Muralidharan, A.; Thomas, S.; Shah, G.; van Soest, R. W.; El Sayed, K. A. *Bioorg.Med.Chem.* **2009**, *17*, 1731.
32. Rodriguez, L. G.; Wu, X.; Guan, J. L. *Methods Mol. Biol.* **2005**, *294*, 23.
33. Omnia Assay Manual, <http://products.invitrogen.com/ivgn/product/KPZ3121>, accessed on December 1, 2012.



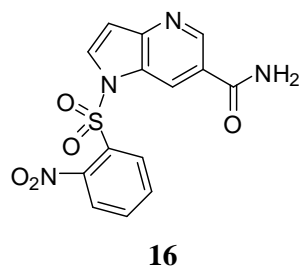
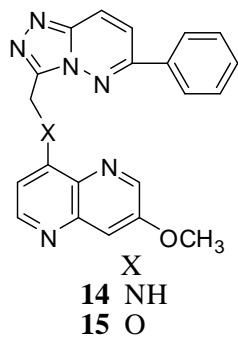
**Scheme 1.** Synthesis of tyrosol ester analogue 7.



**Scheme 2.** Synthesis of tyrosol carbamate analogue 12.



Compound	R <sub>1</sub>	R <sub>2</sub>
3	H	H
4	H	a
5	H	b
6	H	c
7	H	d
8	H	e
9	H	f
10	H	g
11	H	h
12	H	i
13	h	h



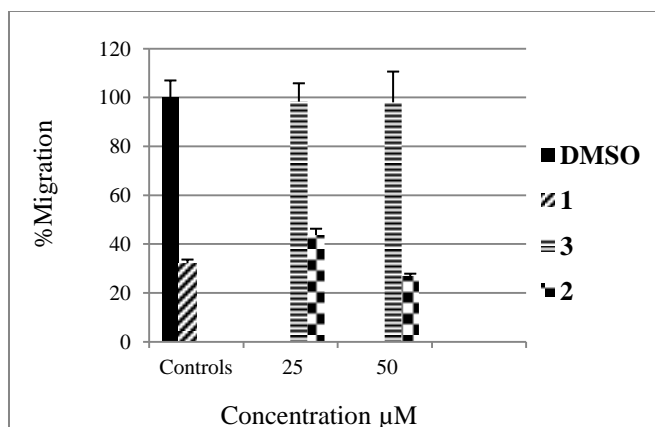


**Figure 1.** Antimigratory activity of **2** and **3** against the human breast cancer cells MDA-MB231. Error bars indicate the SD of  $n = 3$ /dose. DMSO was used as a negative control while **1** was used as a positive control at 10  $\mu\text{M}$  dose.<sup>5</sup>

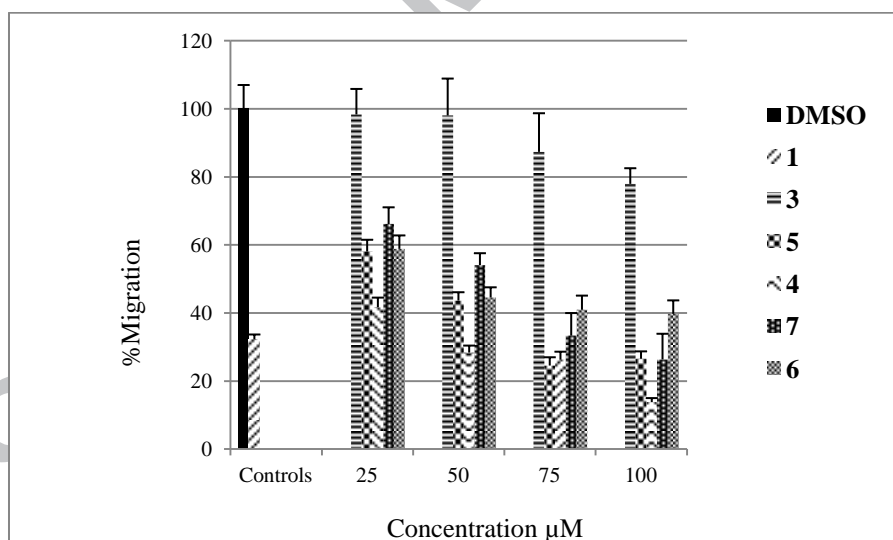


**Figure 2.** Antimigratory activity of **3-7** against the human breast cancer cells MDA-MB231. Error bars indicate the SD of  $n = 3$ /dose. DMSO was used as a negative control while **1** was used as a positive control at 10  $\mu\text{M}$  dose.<sup>5</sup>

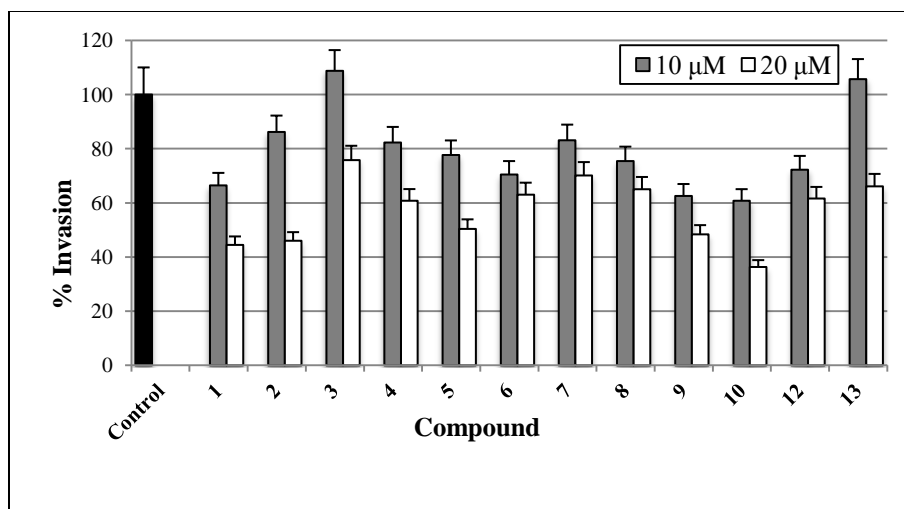


**Figure 3.** Anti-invasive activities of **1-10**, **12**, and **13** against the human breast cancer cell line MDA-MB231 using Cultrex<sup>®</sup> BME cell invasion assay kit. Each concentration was run in triplicate and the data are expressed as the mean $\pm$ SEM. **1** was used as a positive control.<sup>5</sup>

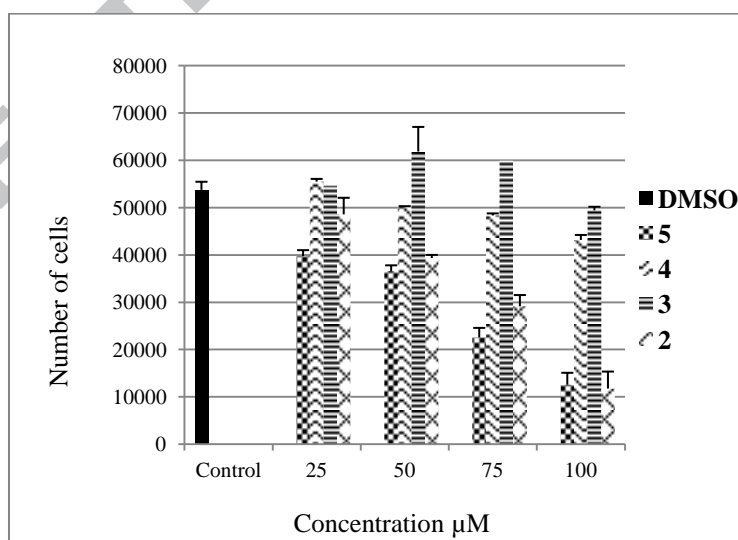


**Figure 4.** Antiproliferative activity of **2-5** against MDA-MB231 cells. Error bars indicate the SD of n = 3/dose.

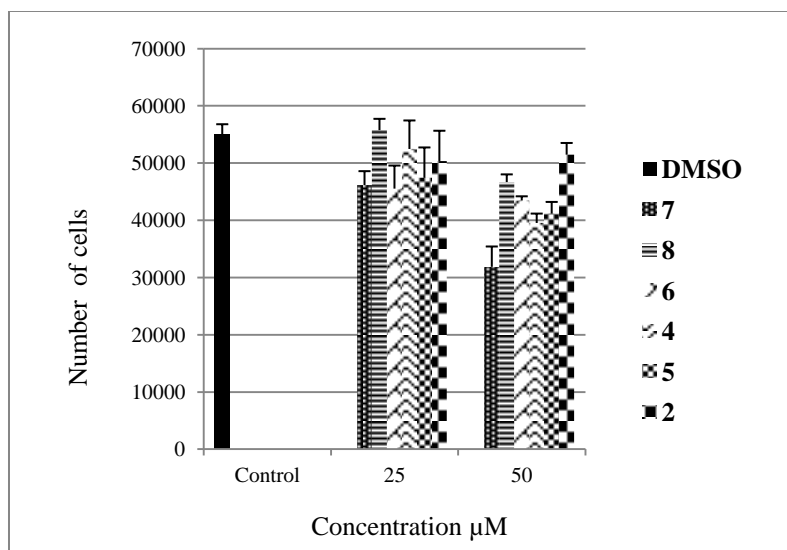


**Figure 5.** Cytotoxic activity of **2-6** against non-tumorigenic human breast MCF10A epithelial cell line. Error bars indicate the SD of  $n = 3/\text{dose}$ .

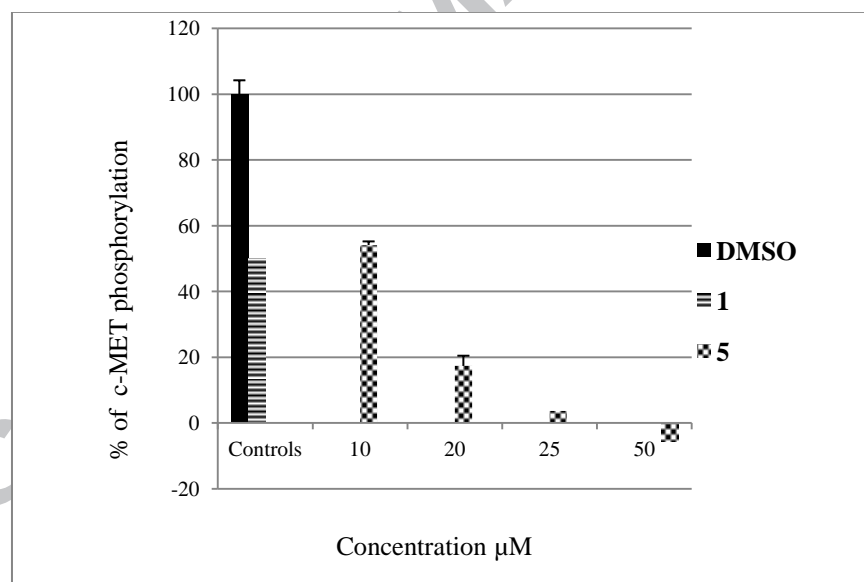
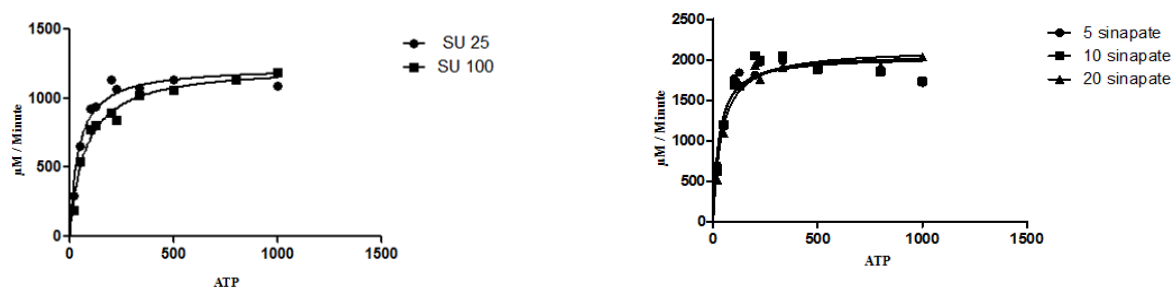


**Figure 6.** Percentage of c-MET phosphorylation by various doses of **5** using Z'-LYTE™ assay kit. Error bars indicate the SD of  $n = 3$  per dose. **1** was used as a positive control.<sup>5</sup>



	SU11274		Analogue 5		
	25 nM	100 nM	5 $\mu$ M	10 $\mu$ M	20 $\mu$ M
$V_{\max}$	1226	1231	2039	2073	2136
$K_m$	41.12	72.55	27.74	30.68	41.02

**Figure 7.** Kinetics of binding of **5** at the ATP binding pocket of c-MET by using Omnia<sup>®</sup> kinase Assay. The known c-MET competitive inhibitor SU11274 was used as a positive control.<sup>20</sup>

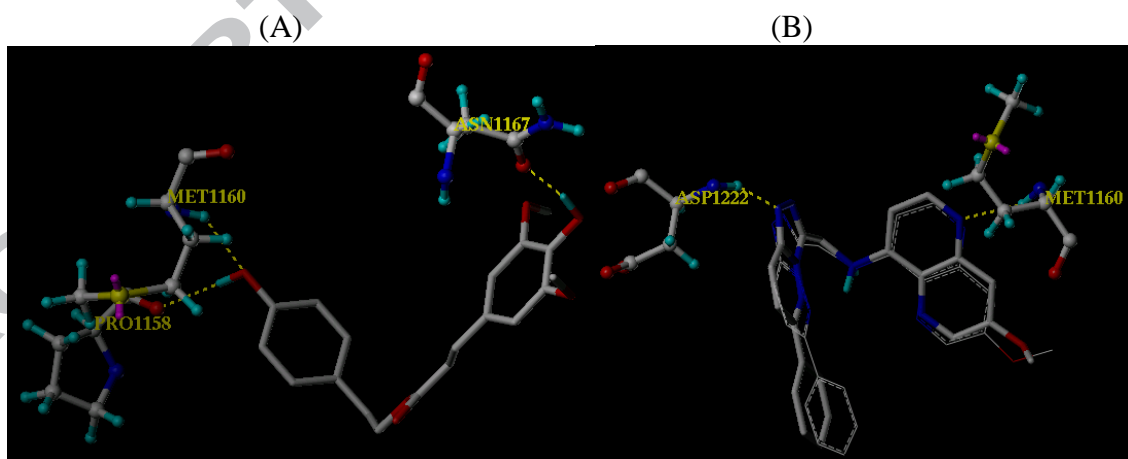


**Figure 8.** A: Important HB interactions of analogue **5** at the ATP binding site of c-MET (PDB 3I5N). B: Overlaid ligand (**14**, white stick) obtained from the crystal structure of c-MET (PDB 3I5N) and the same ligand after the docking simulation (dotted structure).

**Table 1.**  $^1\text{H}$  NMR Data of Compounds **4–8**.<sup>a</sup>

Position	$\delta_{\text{H}}$ ( $J$ in Hz)				
	<b>4</b>	<b>5</b>	<b>6</b>	<b>7</b>	<b>8</b>
2	-	6.26, d (16.0)	3.44, s	6.32, d (15.6)	3.49, s
3	7.19, s	7.56, d (16.0)	-	7.57, d (15.6)	-
4	-	-	6.61, d (1.8)	-	6.69, d (1.5)
5	-	6.72, s	-	6.71, s	-
7	7.19, s	-	6.77, d (7.8)	-	6.83, d (7.8)
8	3.85, s	-	6.64, dd (7.8, 1.8)	-	6.71, dd (7.8, 1.5)
9	3.85, s	6.72, s	-	6.71, s	3.82, s
10	-	3.88, s	-	3.85, s	-
11	-	3.88, s	-	3.86, s	-
12	-	-	-	3.85, s	-
1'	4.41, t (6.6)	4.35, t (7.3)	4.25, t (6.8)	4.36, t (7.4)	4.23, t (6.9)
2'	2.94, t (6.7)	2.91, t (7.3)	2.82, t (6.8)	2.91, t (7.4)	2.81, t (6.9)
4'	6.71, d (8.7)	6.78, d (8.7)	6.72, d (8.7)	6.32, d (8.2)	6.69, d (8.2)
5'	7.10, d (8.7)	7.08, d (8.7)	6.99, d (8.2)	7.08, d (8.2)	6.96, d (8.2)
7'	7.10, d (8.7)	7.08, d (8.7)	6.99, d (8.2)	7.08, d (8.2)	6.96, d (8.2)
8'	6.71, d (8.7)	6.78, d (8.7)	6.72, d (8.7)	6.32, d (8.2)	6.69, d (8.2)

<sup>a</sup>In  $\text{CDCl}_3$ , 400 MHz. Coupling constants ( $J$ ) are in Hz.

**Table 2.**  $^{13}\text{C}$  NMR Data of Compounds **4–8**.<sup>a</sup>

Position	$\delta_{\text{C}}$				
	<b>4</b>	<b>5</b>	<b>6</b>	<b>7</b>	<b>8</b>
1	166.7, qC	167.4, qC	172.3, qC	167.0, qC	171.8, qC
2	120.2, qC	115.7, CH	40.7, $\text{CH}_2$	117.8, CH	41.1, $\text{CH}_2$
3	106.6, CH	145.4, CH	126.5, qC	145.7, CH	125.8, qC
4	147.5, qC	125.9, qC	115.4, CH	129.8, qC	111.7, CH
5	140.5, qC	105.1, CH	142.9, qC	105.9, CH	146.4, qC
6	147.5, qC	147.2, qC	143.5, qC	152.0, qC	144.6, qC
7	106.6, CH	137.2, qC	116.4, CH	139.0, qC	114.4, CH
8	55.4, $\text{CH}_3$	147.2, qC	122.1, CH	152.0, qC	122.1, CH
9	55.4, $\text{CH}_3$	105.1, CH	-	105.9, CH	55.9, $\text{CH}_3$
10	-	56.4, $\text{CH}_3$	-	56.0, $\text{CH}_3$	-
11	-	56.4, $\text{CH}_3$	-	61.0, $\text{CH}_3$	-
12	-	-	-	56.0, $\text{CH}_3$	-
1'	65.5, $\text{CH}_2$	65.3, $\text{CH}_2$	65.5, $\text{CH}_2$	65.6, $\text{CH}_2$	65.6, $\text{CH}_2$
2'	34.0, $\text{CH}_2$	34.2, $\text{CH}_2$	34.3, $\text{CH}_2$	34.2, $\text{CH}_2$	34.2, $\text{CH}_2$
3'	128.9, qC	129.9, qC	129.9, qC	130.2, qC	130.2, qC
4'	115.9, $\text{CH}_2$	115.5, $\text{CH}_2$	115.3, $\text{CH}_2$	115.2, $\text{CH}_2$	115.2, CH
5'	129.6, CH	130.1, CH	130.2, CH	130.1, CH	130.1, CH
6'	155.8, qC	154.5, qC	154.3, qC	154.2, qC	154.2, qC
7'	129.6, CH	130.1, CH	130.2, CH	130.1, CH	130.1, CH
8'	115.9, CH	115.5, CH	115.3, CH	115.2, CH	115.2, CH

<sup>a</sup>In  $\text{CDCl}_3$ , 100 MHz. Carbon multiplicities were determined by APT or PENDANT experiments. C = quaternary, CH = methine,  $\text{CH}_2$  = methylene,  $\text{CH}_3$  = methyl carbons.

**Table 3.**  $^1\text{H}$  NMR Data of Compounds **9–13**.<sup>a</sup>

Position	$\delta_{\text{H}}$ ( $J$ in Hz)				
	<b>9</b>	<b>10</b>	<b>11</b>	<b>12</b>	<b>13</b>
2	6.18, d (16.0)	8.50, s	4.23, d (5.9)	-	4.44, d (5.9)
3	7.46, d (16.0)	-	-	7.85, d (8.7)	-
4	-	-	7.23, m	7.30, d (8.3)	7.23, m
5	6.97, d (1.8)	8.60, d (8.2)	7.33, m	-	7.33, m
6	-	7.24, d (8.2)	7.26, m	7.30, d (8.3)	7.26, m
7	-	-	7.33, m	7.85, d (8.7)	7.33, m
8	6.73, d (8.3)	-	7.23, m	2.42, s	7.23, m
9	6.88, dd (8.3, 1.8)	-	-	-	-
11	-	2.63, s	-	-	-
12	-	4.42, q (7.3)	-	-	-
13	-	1.44, t (7.3)	-	-	-
NH	-	-	5.30, m	-	5.30, m
1'	4.24, t (6.9)	4.42, t (7.8)	3.81, t (6.4)	4.21, t (6.4)	4.28, t (7.8)
2'	2.83, t (6.9)	2.96, t (7.8)	2.83, t (6.4)	2.79, t (6.4)	2.90, t (7.8)
4'	6.67, d (8.2)	6.74, d (8.7)	7.20, d (8.2)	6.71, d (8.3)	7.26, d (8.7)
5'	7.02, d (8.2)	7.11, d (8.7)	7.07, d (8.2)	6.97, d (8.2)	7.24, d (8.7)
7'	7.02, d (8.2)	7.11, d (8.7)	7.07, d (8.2)	6.97, d (8.2)	7.24, d (8.7)
8'	6.67, d (8.2)	6.74, d (8.7)	7.20, d (8.2)	6.71, d (8.9)	7.26, d (8.7)
2''	-	-	-	-	4.34, d (6.0)
3''	-	-	-	-	-
4''	-	-	-	-	7.23, m
5''	-	-	-	-	7.33, m
6''	-	-	-	-	7.26, m
7''	-	-	-	-	7.33, m
8''	-	-	-	-	7.23, m
NH	-	-	-	-	4.93, m

<sup>a</sup>In  $\text{CDCl}_3$ , 400 MHz. Coupling constants ( $J$ ) are in Hz.

**Table 4.**  $^{13}\text{C}$  NMR Data of Compounds **9-13**.<sup>a</sup>

Position	$\delta_{\text{C}}$				
	<b>9</b>	<b>10</b>	<b>11</b>	<b>12</b>	<b>13</b>
1	167.0, qC	-	156.2, qC	155.0, qC	157.0, qC
2	113.8, CH	148.0, CH	45.1, CH <sub>2</sub>	146.0, qC	45.0, CH <sub>2</sub>
3	145.6, CH	112.0, qC	137.9, qC	129.5, CH	138.5, qC
4	126.9, qC	176.0, qC	128.9, CH	128.0, CH	128.8, CH
5	113.8, CH	136.0, CH	127.8, CH	136.0, qC	127.8, CH
6	145.7, qC	122.0, CH	127.8, CH	128.0, CH	127.8, CH
7	148.0, qC	148.0, qC	127.8, CH	129.5, CH	127.8, CH
8	121.0, CH	-	128.9, CH	22.0, CH <sub>3</sub>	128.8, CH
9	114.9, CH	164.0, qC	-	-	-
10	-	121.0, qC	-	-	-
11	-	26.0, CH <sub>3</sub>	-	-	-
12	-	46.0, CH <sub>2</sub>	-	-	-
13	-	15.0, CH <sub>3</sub>	-	-	-
14	-	166.0, qC	-	-	-
1'	65.0, CH <sub>2</sub>	66.0, CH <sub>2</sub>	62.6, CH <sub>2</sub>	68.0, CH <sub>2</sub>	65.3, CH <sub>2</sub>
2'	34.0, CH <sub>2</sub>	35.0, CH <sub>2</sub>	34.2, CH <sub>2</sub>	34.0, CH <sub>2</sub>	34.8, CH <sub>2</sub>
3'	128.0, qC	128.0, qC	130.8, qC	129.0, qC	135.1, qC
4'	115.2, CH	116.0, CH	130.2, CH	116.0, CH	129.7, CH
5'	129.0, CH	130.0, CH	115.8, CH	130.0, CH	121.6, CH
6'	155.0, qC	156.0, qC	155.7, qC	151.0, qC	149.6, qC
7'	129.0, CH	130.0, CH	115.8, CH	130.0, CH	121.6, CH
8'	115.2, CH	116.0, CH	130.2, CH	116.0, CH	129.7, CH
1''	-	-	-	-	155.2, qC
2''	-	-	-	-	44.9, CH <sub>2</sub>
3''	-	-	-	-	138.1, qC
4''	-	-	-	-	128.7, CH
5''	-	-	-	-	127.5, CH
6''	-	-	-	-	127.5, CH
7''	-	-	-	-	127.5, CH
8''	-	-	-	-	128.7, CH

<sup>a</sup>In CDCl<sub>3</sub>, 100 MHz. Carbon multiplicities were determined by APT or PENDANT experiments.

C = quaternary, CH = methine, CH<sub>2</sub> = methylene, CH<sub>3</sub> = methyl carbons.

**Table 5.** c-MET inhibitory activities of **1-10** and **12-13** in Z'-Lyte™ kinase assay at 25µM dose.

Compound	% Phosphorylation Inhibition
<b>1</b> <sup>a</sup>	93.4
<b>2</b>	4.2
<b>3</b>	0
<b>4</b>	6.4
<b>5</b>	95.5
<b>6</b>	0
<b>7</b>	0
<b>8</b>	13.1
<b>9</b>	22.4
<b>10</b>	0
<b>12</b>	0
<b>13</b>	0

<sup>a</sup>Used dose 10 µM.

**Table 6.** IC<sub>50</sub> Values of **1-13** using the MTT and WHA assays against MDA-MB231 cells.

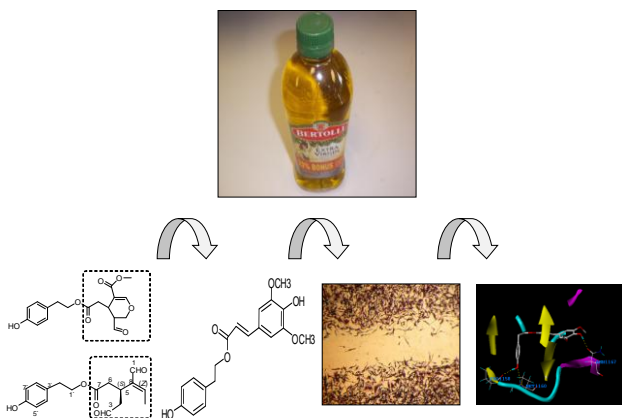
Compound	MTT assay (IC <sub>50</sub> , µM)	WHA (IC <sub>50</sub> , µM)
<b>1</b>	15 <sup>a</sup>	7.5
<b>2</b>	80.4	13.8
<b>3</b>	>100	>100
<b>8</b>	>100	>100
<b>10</b>	>100	>100
<b>6</b>	>100	41.6
<b>9</b>	>100	>100
<b>5</b>	73.7	33.5
<b>4</b>	>100	19.4
<b>7</b>	>100	46.7
<b>13</b>	>100	>100
<b>11</b>	>100	>100
<b>12</b>	>100	>100

<sup>a</sup>Reported IC<sub>50</sub> of **1** in MTT assay.<sup>5</sup>

## Table of Content Graphic

### Olive Secoiridoids and Semisynthetic Bioisostere Analogues for the Control of Metastatic Breast Cancer

Belnaser A. Busnena, Ahmed I. Foudah, Tina Melancon, and Khalid A. El Sayed\*



## Olive Secoiridoids and Semisynthetic Bioisostere Analogues for the Control of Metastatic Breast Cancer

Belnaser Busnena, Ahmed I. Foudah, Tina Melancon, and Khalid A. El Sayed

Department of Basic Pharmaceutical Sciences, College of Pharmacy,  
University of Louisiana at Monroe, Monroe, LA 71201.

